Disproportionation of Iron(III) Porphyrin π-Cation Radicals in the Presence of Sterically Hindered Pyridines. Spectroscopic Detection of Asymmetric Highly Oxidized Intermediates

Krystyna Rachlewicz and Lechosław Latos-Grażyński*

Department of Chemistry, University of Wrocław, 50 383 Wrocław, Poland

Received July 13, 1995[⊗]

The reactivity of iron(III) tetraphenylporphyrin π-cation radical (TPP$^{\bullet}$)Fe^{III}(ClO$_4$)$_2$, (**1**-1) iron(III) tetra-*p*-tolylporphyrin π-cation radical (TTP$^{\bullet}$)Fe^{III}(ClO$_4$)$_2$ (**1**-2) and iron(III) tetramesitylporphyrin π-cation radical (TMP$^{\bullet}$)-Fe^{III}(ClO$_4$)$_2$ (**1**-3) complexes with 2,4,6-collidine, 2,3,6-collidine, 2-picoline, 2,6-di-*tert*-butylpyridine, and 2,6-dibromopyridine has been examined by ^{1}H NMR spectroscopy in dichloromethane-d_2 solution at low temperatures. These complexes undergo hydration processes which are essential in the generation of highly oxidized species via acid base/equilibria of coordinated water followed by disproportionation pathway, giving as sole stable products [(TPP$^{\bullet}$)Fe^{III}OFe^{III}(TPP)]$^+$ (**4**-1), [(TTP$^{\bullet}$)Fe^{III}OFe^{III}(TTP)]$^+$ (**4**-2), and (TMP)Fe^{III}(OH) (**6**) respectively. The sterically hindered pyridines act as efficient proton scavengers. Two novel highly oxidized iron complexes have been detected by ^{1}H NMR spectroscopy after addition of 2,4,6-collidine to (TTP$^{\bullet}$)Fe^{III}(ClO$_4$)$_2$ or (TPP$^{\bullet}$)Fe^{III}(ClO$_4$)$_2$ in dichloromethane-d_2 solution at 202 K. New intermediates have been identified as iron porphyrin *N*-oxide complexes, i.e., iron(III) porphyrin *N*-oxide cation radical (**2**-*n*) and iron(IV) porphyrin *N*-oxide radical (**3**-*n*). The ^{1}H NMR results indicate that the D_{4h} symmetry of the parent iron(III) π-cation radical is drastically reduced upon disproportionation in the presence of proton scavengers. Both species are very unstable and were observed from 176 to 232 K. The intermediate **2**-2 has a ^{1}H NMR spectrum which demonstrates large hyperfine shifts (ppm) for the meso *p*-tolyl substituents (ortho 98.0, 94.8, 92.9, 91.7; meta −34.8, −38.7, −41.5, −42.3; *p*-CH$_3$ −86.3, −88.0) which are consistent with presence of an N-substituted iron porphyrin radical in the product mixture. The characteristic ^{1}H NMR spectrum of **2**-2 includes six pyrrole resonances at 149.6, 118.2, 115.4, 88.3, 64.6, and 55.7 ppm at 202 K, i.e., in the positions corresponding to iron(III) high-spin porphyrins. On warming to 222 K, the pyrrole resonances broaden and then coalesce pairwaise. Such dynamic behavior is accounted for by a rearrangement mechanism which involves an inversion of the porphyrin puckering. The pattern of *p*-tolyl resonances revealed the cation radical electronic structure of **3**-2. The *p*-tolyl resonances are divided in two distinct sets showing opposite direction of the isotropic shift for the same ring positions. The pyrrole resonances of **3**-2 also demonstrated downfield and upfield shifts. A disproportionation mechanism of the hydrated iron porphyrin cation radicals to generate **2** and **3** has been proposed. Both intermediates react with triphenylphosphine to produce triphenylphosphine oxide and high-spin iron porphyrins. Addition of 2,4,6-collidine to (TMP$^{\bullet}$)Fe^{III}-(ClO$_4$)$_2$ does not produce analogs of **2** and **3** found for sterically unprotected porphyrins. It results instead in the formation of a variety of X(TMP$^{\bullet}$)Fe^{IV}O (**5**) complexes also accounted for by the disproportionation process.

Introduction

Intense interest in iron porphyrin π-cation radicals has been stimulated by their involvement in various biological processes or in catalytic reactions of metalloporphyrins.[1,2] Several different patterns of the reactivity of iron(III) porphyrin π-cation radical complexes have been established. Outer sphere, one-electron transfer from bromide, iodide, or 1,8-bis(dimethylamino)naphthalene resulted in formation of iron(III) porphyrin complexes.[3] In the presence of bases with a high oxidation potential (e.g. pyridine), formation of a radical form of the (μ-oxo)diiron(III) complex [(TPP)Fe^{III}−O−Fe^{III}(TPP$^{\bullet}$)]$^+$ was reported.[3] Imidazole ligands converted the high-spin iron(III) porphyrin π-cation radical to a low-spin iron(III) porphyrin π-cation radical.[4] Addition of imidazole also induced a reduction of the iron(III) porphyrin cation radical to the bis(imidazole) low-spin iron(III) porphyrin complex.[4] Contribution of an iron-(III) tetraphenylporphyrin π-cation radical in generation of iron-(III) porphyrins modified at the periphery has been implied in the following reactions: (a) (TPP)Fe^{III}Cl with NO$_2$ to produce (2-NO$_2$TPP)Fe^{III}Cl,[5] (b) (OEP)Fe^{III}Cl with NO$_2$ to produce (5-NO$_2$-OEP)Fe^{III}Cl,[6] and (c) (TPP)Fe^{III}Cl with benzoyl peroxide to give (2-benzoyloxy-TPP)Fe^{III}Cl.[7] Two equivalents of hydroperoxide oxidizes iron(III) tetrarylporphyrin to the corresponding iron(III) isoporphyrin.[8] Previously we have demonstrated that the addition of two relatively easily oxidizable nucleophiles (triphenylphosphine and nitrite anion) to the iron-(III) tetraphenylporphyrin π-cation radical (TPP$^{\bullet}$)Fe^{III}(ClO$_4$)$_2$ resulted in the formation of the β-substituted derivatives, (2-PPh$_3$TPP)Fe^{III}Cl$_2$ and (2-NO$_2$TPP)Fe^{III}Cl, respectively.[9] An interesting reactivity route of iron porphyrin π-cation radical involves internal electron transfer. Coordination of methoxide

* To whom correspondence should be addressed.

[⊗] Abstract published in *Advance ACS Abstracts,* February 1, 1996.

(1) Dunford, H. B. In *Peroxidase in Chemistry and Biology*; Everse, J., Everse, K. E., Grisham, M. B., Eds.; CRC Press: Boca Raton FL, 1991; Vol. II p 1.
(2) McMurry, T. J.; Groves, J. T. In *Cytochrome P-450, Structure, Mechanism and Biochemistry*; Ortiz de Montellano, P. R., Ed.; Plenum Press: New York, 1986; p 1.
(3) (a) Arena, F.; Gans, P.; Marchon, J.-C. *J. Chem. Soc., Chem. Commun.* **1984**, 196. (b) Arena, F.; Gans, P.; Marchon, J.-C. *Nouv. J. Chim.* **1985**, *9*, 505.
(4) Goff, H. M.; Phillippi, M . A. *J. Am. Chem. Soc.* **1983**, *105*, 7567.
(5) Catalano, M. M.; Crossley, M. J.; Harding, M. M.; King, L. G. *J. Chem. Soc. Chem. Commun*. **1984,** 1535.
(6) Fanning, J. C.; Mandel, F. S.; Gray, T. L.; Datta-Gupta, N. *Tetrahedron* **1979**, *39*, 1251.
(7) Wojaczyński, J.; Latos-Grażyński, L. *Inorg. Chem.* **1995,** *35,* 1044.
(8) Gold, A.; Ivey, W.; Toney, G. E.; Sangaiah, R. *Inorg. Chem.* **1984**, *23*, 2932.
(9) Małek, A.; Latos-Grażyński, L.; Bartczak, T. J.; Żądło, A. *Inorg. Chem.* **1991**, *30*, 3222.

0020-1669/96/1335-1136$12.00/0

to the iron(III) tetramesitylporphyrin cation radical $(TMP^{\bullet})Fe^{III}(ClO_4)_2$ resulted in the conversion to the iron(IV) porphyrin $(TMP)Fe^{IV}(OCH_3)_2$.[10] Stabilization of iron(IV) porphyrin was suggested due to coordination of two fluoride anions.[11] Stable oxoiron(IV) porphyrins were conveniently prepared by ligand methathesis of iron(III) porphyrin π-cation radicals carried out over moist basic alumina.[12] Furthermore, the disproportionation of oxoiron(IV) or dimethoxyiron(IV) porphyrins to generate the oxoiron(IV) porphyrin π-cation radical was established.[12]

A mechanism of electrochemical generation of highly oxidized oxoiron(IV) porphyrins by oxidation of hydroxyiron(III) porphyrins involves oxidation of the porphyrin macrocycle followed by an internal electron transfer.[12,13] Addition of an aryl Grignard reagent to an iron(III) tetraphenylporphyrin π-cation radical yielded a σ-aryliron(IV) tetraphenylporphyrin presumally via an inner conversion $\{[(TPP^{\bullet})Fe^{III}Ar]^+\} \rightarrow \{[(TPP)Fe^{IV}Ar]^+\}$.[14] The iron(III) tetramesitylporphyrin cation radical $[(TMP^{\bullet})Fe^{III}](ClO_4)_2$ was used as a convenient outer sphere one-electron oxidizing agent to generate $[(TMP^{\bullet})Fe^{IV}O]$ from $(TMP)Fe^{IV}O$.[15]

Earlier investigations demonstrated that hydration of one-electron oxidized iron(III) porphyrins are essential in the generation of highly oxidized species by way of acid base equilibria and plausible disproportionation pathways.[10,12,13,16,17] The acid/base chemistry seems to be instrumental in interconversion of oxoiron(III) porphyrin dication, iron(III) porphyrin *N*-oxide and iron(III) *N*-hydroxide porphyrin.[18] These species are alternative to oxoiron(IV) porphyrin π-cation radical members of two-electron oxidized ion(III) porphyrins family. In associated systems, three isoelectronic structures of one-electron oxidized nickel porphyrins were considered to account for the reaction of nickel(II) porphyrin *N*-oxide with acid.[19]

Recently we have found that the hydrated iron(III) porphyrin π-cation radical plays a triple role in the iron(III) porphyrin π-cation radical−pyridine system.[16] It acts as an electrophilic substrate, as a one-electron oxidizing reagent, and as a proton donor. Simultaneously, pyridine acts as an nucleophilic reagent and a proton scavenger. We have presented evidence for the reaction of the porphyrin ring with pyridine with formation of stable β-pyridiniumtetraphenylporphyrin and unstable 5-pyridiniumylisotetraphenylporphyrin and 5,15-dipyridiniumyltetraphenylporphodimethene iron complexes.

Considering the rich chemistry demonstrated for the iron(III) porphyrin π-cation radical−pyridine system, we have decided to inhibit the formation of meso- and β-substituted intermediates by using sterically hindered substituted pyridines such as 2-picoline, 2,6-di-*tert*-butylpyridine, 2,3,6-collidine, 2,4,6-collidine, and 2,6-dibromopyridine.

We have focused the research on highly oxidized intermediates of the process formed under such exceptionally oxidizing conditions. In order to facilitate the detection of reaction products and to gain a better understanding of their properties in solution, we have undertaken systematic ^{1}H NMR investigations, taking advantage of the fact that this spectroscopy provides an extremely useful probe for direct study of the structure and chemistry of paramagnetic ion porphyrins under such experimental conditions. The hyperfine shift patterns are particularly sensitive to the symmetry, spin/electronic, and ligation states of iron porphyrins[20] including coordination core modified ones.[18,21−23]

By carrying out the ^{1}H NMR titration of iron(III) porphyrin π-cation radicals at low temperatures in an inert solvent (dichloromethane-d_2), we have detected novel highly oxidized intermediates formed during the disproportionation process. Their spectroscopic features have been accounted for by a modification of the coordination porphyrin core inherently associated with the π-cation radical electronic structure of the generated highly asymmetric macrocycle.

Results

Reaction of Iron(III) Tetraphenylporphyrin Cation Radical $(TPP^{\bullet})Fe^{III}(ClO_4)_2$ with 2,4,6-Collidine. The titration of $(TPP^{\bullet})Fe^{III}(ClO_4)_2$ (**1**-1) with 2,4,6-collidine was followed by ^{1}H NMR; representative spectra are presented in Figure 1. When 0.5 equiv of 2,4,6-collidine is added, a new species, **2**-1, with a new ^{1}H NMR spectrum begins to form; 2 equiv of 2,4,6-collidine is required for optimal conditions to generate this intermediate. The resonances characteristic of $[(TPP^{\bullet})Fe^{III}OFe^{III}(TPP)]^+$ (**4**-1) can be easily observed.[3] The further addition of 2,4,6-collidine up to a 1:6 molar ratio does not change the chemical shifts although some broadening of resonances was observed. The molar ratio of the new intermediate (**2**-1) to the final reaction product $[(TPP^{\bullet})Fe^{III}OFe^{III}(TPP)]^+$ (**4**-1) equals ca. 1:1.7 as found by deconvolution of the NMR spectrum. Additionally the monomeric high-spin iron porphyrin $((TPP)Fe^{III}X)$ was usually observed. Trace A in Figure 1 shows the spectrum resulting from the observation of dichloromethane-d_2 solution of **1**-1 after the addition of 2 equiv of 2,4,6-collidine. A new species **2**-1 is present whose resonances extend from +160 to −50 ppm. The individual resonances have been assigned through labeling experiment and consideration of relative intensities. The following starting species were used for the analysis: $(TPP^{\bullet})Fe^{III}(ClO_4)_2$, **1**-1; $(TPP\text{-}d_8^{\bullet})Fe^{III}(ClO_4)_2$, **1**-1$-d_8$; $(TPP\text{-}d_{20}^{\bullet})Fe^{III}(ClO_4)_2$, **1**-1$-d_{20}$; $(TTP^{\bullet})Fe^{III}(ClO_4)_2$, **1**-2; $(TTP\text{-}d_8^{\bullet})Fe^{III}(ClO_4)_2$, **1**-2$-d_8$.

The ^{1}H NMR spectra of the **2**-1-d_{20} intermediate, deuterated selectively at the *meso*-phenyl positions, collected at several

(10) (a) Groves, J. T.; Quinn, R.; McMurry, T. J.; Nakamura, M.; Lang, G.; Boso, B. *J. Am. Chem. Soc.* **1985**, *107*, 354. (b) Groves, J. T.; McMurry, T. J. *Rev. Port. Quim.* **1985,** *27*, 102.
(11) Hickman, D. L.; Nanthakumar, A.; Goff, H. M. *J. Am. Chem. Soc.* **1988**, *110*, 6384.
(12) Groves, J. T.; Gross, Z.; Stern, M. K. *Inorg. Chem.* **1994**, *33*, 5065.
(13) (a) Calderwood, T. S.; Lee, W. A.; Bruice, T. C. *J. Am. Chem. Soc.* **1985**, *107*, 8272. (b) Lee, W. A.; Calderwood, T. S.; Bruice, T. C. *Proc. Natl. Acad. Sci. U.S.A.* **1985**, *82*, 4301. (c) Groves, J. T.; Gilbert, J. A. *Inorg. Chem.* **1986**, *25*, 125. (d) Calderwood, T. S.; Bruice, T. C. *Inorg. Chem. 1986*, *25*, 3722. (e) Swistak, C.; Mu, X. H.; Kadish, K. M.; *Inorg. Chem.* **1987**, *26*, 4360.
(14) Chmielewski, P. J.; Latos-Grażyński, L.; Rachlewicz, K. *Magn. Reson. Chem* **1993**, *31*, S47.
(15) Balch, A. L.; Latos-Grażyński, L; Renner, M. W. *J. Am. Chem. Soc.* **1985**, *107*, 2983.
(16) Rachlewicz, K.; Latos-Grażyński, L. *Inorg. Chem.* **1995**, *34*, 718.
(17) (a) Ivanca, M. A.; Lappin, A. G.; Scheidt, W. R. *Inorg. Chem.* **1991**, *30*, 711. (b) Rodgers, K. R.; Reed, R. A.; Su, Y. O; Spiro, T. G. *Inorg. Chem.* **1992**, *31*, 2688.
(18) Tsurumaki, H.; Watanabe, Y.; Morishima, I. *J. Am. Chem. Soc.* **1993**, *115*, 11784.
(19) Tsurumaki, H.; Watanabe, Y.; Morishima, I. *Inorg. Chem.* **1994**, *33*, 4186.
(20) (a) La Mar, G. N.; Walker (Jensen), F. A. In *The Porphyrins*; Dolphin, D., Ed.; Academic Press: New York, 1978; Vol. 4, p 61. (b) Bertini, I.; Luchinat, C. *NMR of Paramagnetic Molecules in Biological Systems*; The Benjamin/Cummings Publishing Company: Reading, MA, 1986. (c) Walker, F. A., Simonis, U. In *Biological Magnetic Resonance*; Berliner, L. J., Reuben, J., Eds.; NMR of Paramagnetic Molecules 12; Plenum Press: New York, 1993; p 133.
(21) (a) Groves, J. T.; Watanabe, Y. *J. Am. Chem. Soc.* **1986**, *108*, 7836. (b) Groves, J. T.; Watanabe, Y. *J. Am. Chem. Soc.* **1988**, *110*, 8443.
(22) (a) Balch, A. L.; Chang, Y. W.; La Mar, G. N.; Latos-Grażyński, L.; Renner, M. W. *Inorg. Chem.* **1985**, *24*, 1437. (b) Balch; A. L; Cheng; R.-J.; La Mar; G. N.; Latos-Grażyński, L. *Inorg. Chem.* **1985**, *24*, 2651. (c) Balch, A. L.; La Mar, G. N.; Latos-Grażyński, L.; Renner, M. W. *Inorg Chem.* **1985**, *24*, 2432. (d) Balch, A. L.; Cornman, C. R.; Latos-Grażyński, L.; Olmstead, M. M. *J. Am. Chem. Soc.* **1990**, *112*, 7552.
(23) Balch, A. L.; Cornman, C. R.; Latos-Grażyński, L.; Renner, M. W. *J. Am. Chem. Soc.* **1992**, *114*, 2230.

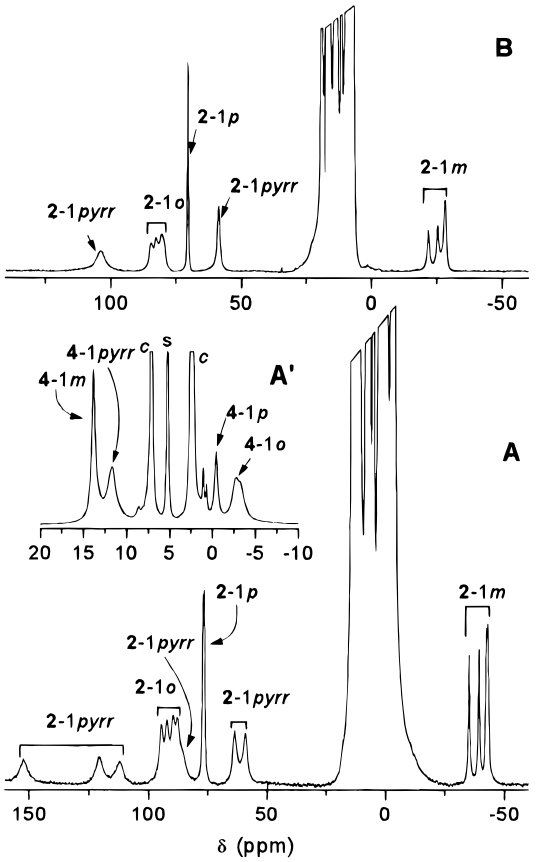

Figure 1. 300 MHz spectra of a dichloromethane-d_2 solution of (TPP•)-$Fe^{III}(ClO_4)_2$ after addition of 2 equiv of 2,4,6-collidine (A) at 202 K or (B) at 232 K. Inset in trace A′ presents an expansion of the +20 to −10 ppm region. Compounds are labeled as in the text; subscripts refer to assignments: pyrr, porphyrin pyrrole protons; o, m, p, ortho, meta, para phenyl protons; s, solvent; c, 2,4,6-collidine.

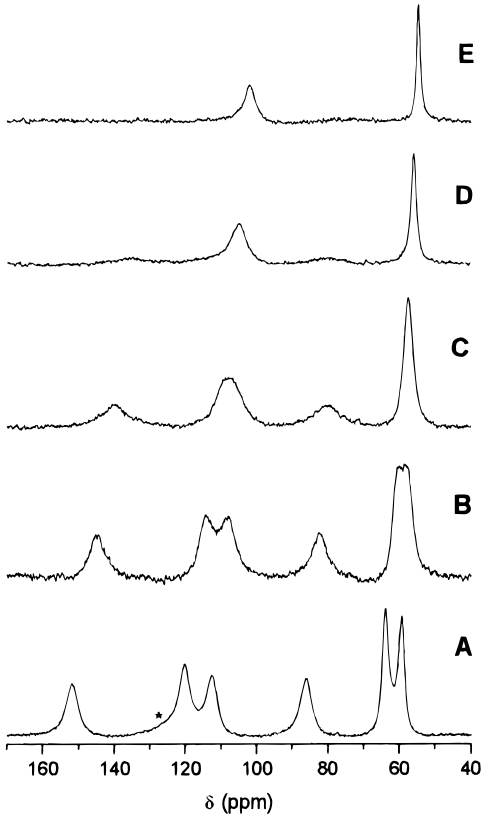

Figure 2. Temperature dependent 300 MHz ^{1}H NMR spectra of the intermediate **2**-1 formed from (TPP•-d_{20})$Fe^{III}(ClO_4)_2$ by addition of 2 equiv of 2,4,6-collidine in dichloromethane-d_2: (A) 202 K, (B) 207 K, (C) 212 K, (D) 217 K, and (E) 222 K. The resonance marked by an asterisk in trace A corresponds to the high-spin iron(III) porphyrin complex (TPP-d_{20})Fe^{III}X.

temperatures including those shown for **2**-1 in Figure 1, are presented in Figure 2. The six downfield pyrrole resonances, assigned on the basis deuterium labeling studies and comparison to the **2**-1-d_8 spectrum (not shown), are particularly evident. The remaining resonances of **2**-1 in Figure 1 are assigned to meso phenyl groups. The four resonances of comparable line width in the 100−80 ppm range are assigned to the ortho phenyl protons, four other identified in the −20 to −40 ppm range are due to the four inequivalent meta phenyl protons. Finally, the remaining two narrowest resonances, centered at 77 ppm, have been assigned to para phenyl protons. The comparisons of the spectra obtained for **2**-1 and **2**-2 (vide infra) resulted in an identification of two *p*-methyl resonances. In **2**-2, the downfield shifted para resonaces of **2**-1 (76.7, 77.1 ppm) have been replaced by upfield shifted *p*-methyl resonances (−86.3; −88.0 ppm). The line widths of the phenyl resonances increase in the range ortho > meta > para as expected for the dipolar contribution to the relaxation mechanism which is presumed to be proportional to r^{-6} where r is the distance from the iron to the proton in question.[20] However the sign alternation of the phenyl resonances and the size of the isotropic shifts indicates the considerable π spin density at the meso phenyl positions.

The ^{1}H NMR spectral parameters for **2**-1 and other relevant iron porphyrin including iron N-substituted porphyrin complexes are collected in Table 1. The meticulous deconvolutions at several different temperatures were carried out to establish rather untypical intensity ratios. Consequently, each pyrrole resonance corresponds to one proton. Relative intensities of each identified ortho, meta, and para resonances are also corresponding to intensity of the one proton. A preliminary analysis on the presumption that the novel intermediate has C_1 geometry requires eight unequivalent pyrrole resonances and four unequivalent meso phenyls each corresponding to two ortho, two meta, and one para proton resonances. Restricted rotation about the meso carbon−phenyl bond and the inequivalence of the two sides of the porphyrin produce differentiation of the ortho and meta resonances. In spite of considerable effort, we could not trace the two missing pyrrole resonances as well as resonances corresponding to two other meso phenyls even over the range +1000 to −1000 ppm. It is likely that some of the resonances occur under the strong resonances of the dominant reaction product $[(TPP^{\bullet})Fe^{III}OFe^{III}(TPP)]^+$ and 2,4,6-collidine or are too broad to be observed. In this respect one has to notice the peculiar temperature dependence of the line widths of two pyrrole resonances at 152.5 and 85.4 ppm (202 K) which are practically removed from the resonance count at 222 K. The **2**-1 species can be only observed over the limited temperature range 177−232 K in dichloromethane-d_2 and chloroform-*d*. It undergoes fast decomposition at 232 K, but gradual decomposition has been seen at 203 K as well. Plots of the chemical shifts vs 1/T shown in Figure 3 reveal that all resonances seen for the **2**-1 intermediate demonstrate some deviations from the typical Curie behavior because the linear extrapolation shows considerable deviation from the anticipated diamagnetic positions at infinite temperature.

The spectral pattern of **2**-1 is temperature dependent as shown in Figures 1 and 2. The six well-defined pyrrole resonances are observed at 203 K and below. On warming to 222 K the pyrrole resonances broaden and then coalesce pairwaise (120.7 and 112.8; 63.9 and 59.4 ppm at 202 K) due to a common dynamic process discernible in the upper temperature of the stability limits. The two pyrrole resonances with the largest

Table 1. ^{1}H NMR Data for Iron Porphyrin Complexes

compound	chem shift, δ (ppm) pyrr	*o*-Ar	*m*-Ar	*p*-Ar	T (K)	ref
2-1	152.5, 85.4, 120.7, 112.8, 63.9, 59.4	94.8, 92.4, 89.9, 88.1	−35.0, −39.2, −42.4, −42.8	77.1, 76.7	203	*a*
2-2	149.6,[b] 118.2, 115.4, 88.3, 64.6, 55.7	98.0, 94.8, 92.9, 91.7	−34.8, −38.7, −41.5, −42.3	(−86.3, −88.0)	203	*a*
2-2′	159.0, 125.7	108.9, 105.8, 102.2, 102.2	−38.2, −42.4, −47.4, −49.3	−105.0, −109.3	203	*a*
3-2[c]	35.9, 28.0, 27.8, 21.7, −8.6, −17.9	A, B, −21.5; C, 25.8, 24.1; D, 25.6, 23.5	A, 21.7, 20.4; B, 23.67, 19.9; C, −3.0, −3.5; D, −4.3, −4.4	A (34.8); B (33.7); C (−18.4); D (−18.7)	203	*a*
1-4[d]	100.2	(−14.4, −18.6)	−56.0	(−8.5)	203	*a*
5-1	−22.4	(26.0, 23.2)	69.0, 67.4	(12.4)	203	*a*
5-2	−18.4	(21.9, 18.9)	55.1, 52.1	(11.0)	203	*a*
TMP-d_8−NOFe^{III}	145, 124, 82, 48				193	18
TMP−NOFe^{III}			17.2, 15.0, 13.8	(4.2)(3.9)	223	21
(*N*-MeTTP)Fe^{II}Cl	41.9, 31.7, −0.3, −0.4	14.6, 6.5, 5.1, 4.3	9.4, 9.3, 8.5, 6.8	8.3, 6.6	296	22a
(TPP)(VC)Fe^{III}Cl[e]	21.5, −21.2, −29.3, −42.3	11.1, 7.8, 12.7, 9.0	10.5, 8.7, 8.8, 8.0	8.7, 7.7	298 K	22b
[*N*-MeTTP)Fe^{III}Cl]$^+$	128, 92, 79, 2		17.4, 16.2, 14.8, 12.8	6.2 (8.1), −0.4 (17.2)	223	22c
[*N*-MeTTP)Fe^{III}(CN)$_2$]$^-$	0.0, −31.5, −34.2, −56.9				183	22
(CD$_3$O)(*N*-MeTTP)Fe^{IV}O	−1.6, −6.3, −7.6, −17.1		9.8, 10.5 (2), 11.0			23
(*N*-MeTTP$^•$)FeX	−152	−72.5, −74.3(2), −76.2	58.8, 58.2, 49.7, 47.7	(125.8, 100.8)	183	23
(TTP$^•$)Fe^{III}(ClO$_4$)$_2$	31.6	−16.6	31.6	31.6	293	*a*
[(TTP$^•$)Fe^{III}Cl](SbCl$_6$]	98.9	78.5, 71.1	−29.7, −31.2	61.7	203	16
(TMP$^•$)Fe^{IV}O	−27	(26, 24)	68	(11.1)	196	15

[a] This paper. [b] Line widths of pyrrole resonances: 1160, 850, 1170, 1045, 560, 560 Hz begining from the most downfield shifted (202 K). [c] Four sets of *p*-tolyl resonaces (A−D) have been identified using the COSY experiment (in parentheses, *p*-CH$_3$ shifts). [d] Two very similar spectra overlayed—the positions for the dominating species are given. [e] VC = [C═C(*p*-C$_6$H$_4$Cl)$_2$].

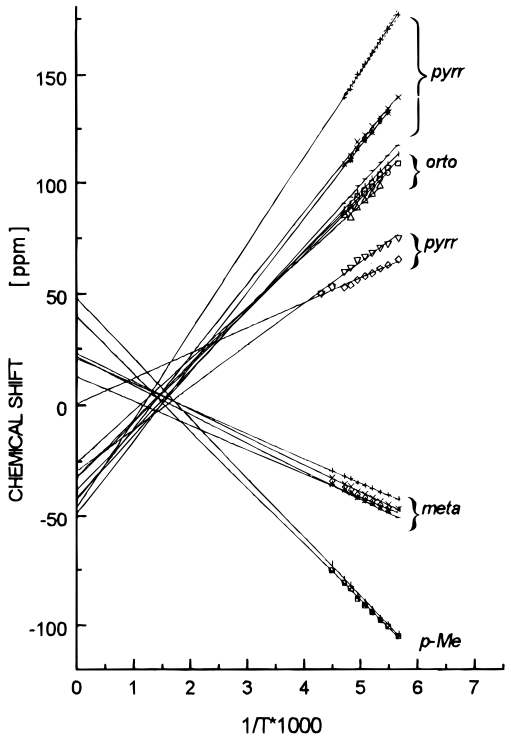

Figure 3. Temperature dependence of chemical shifts for the intermediate **2**-1 formed from **1**-1 by addition of 2 equiv of 2,4,6-collidine in dichloromethane-d_2. The solid line shows the extrapolation of the experimental data points as expected from the Curie law. Labels follow those in Figure 1.

shift differences broaden beyond detection at 222 K. Thus, deceptively simplified spectra are encountered at 232 K with two pyrrole resonances and meso phenyl resonances accountable for by only two phenyl rings (Figure 1). While the intermediate **2**-1 has no symmetry at 203 K, it appears to present an ^{1}H NMR spectrum at 232 K consistent with the effective C_s symmetry. The observation suggests an rearrangement process that is fast on the NMR time scale at this temperature (vide infra). These dynamic spectral changes could be reversed after cooling back to 203 K (not shown) in spite of the considerable decomposition of the intermediate **2**-1 at 232 K. Meanwhile the multiplicity of the phenyl (*p*-tolyl) resonances remains unaltered at 232 K even though the largest shift differences at 202 K of the ortho (6.7 ppm), meta (7.8), and *p*-CH$_3$ (1.7 ppm) resonances are comparable to the shift differences measured for the pyrrole resonances (7.9 or 4.5 ppm). The rearrangement process should average the chemical shifts of phenyl resonances giving an analogous spectral simplification as established for the pyrrole resonances. The spectral consequences of the rearrangement process require large shift separations between phenyls exchanging mutually their structural positions in the course of the above introduced dynamic process. It implies the very large isotropic shifts' differences for phenyls observed and not observed directly in the ^{1}H NMR spectrum of **2**.

Reaction of Iron(III) Tetra-*p*-tolylporphyrin Cation Radical (TTP$^•$)Fe^{III}(ClO$_4$)$_2$ with 2,4,6-Collidine. The titration of **1**-2 with 2,4,6-collidine has been followed by ^{1}H NMR; representative spectra are presented in Figures 4 and 5. The solubility of **1**-2 is markedly higher than **1**-1. This relatively minor substitution, i.e., the replacement of meso phenyls by *p*-tolyl substituents, plays an unexpectedly profound role in fine tuning of the process pathways. The cation radical undergoes hydration in dichloromethane by residual water to give [(TTP$^•$)Fe^{III}(H$_2$O)(ClO$_4$)](ClO$_4$) and [(TTP$^•$)Fe^{III}(H$_2$O)$_2$](ClO$_4$)$_2$ accompanied by acid−base equilibria.[3,16] Under our experimental conditions, lowering the temperature results in transformation of the typical iron(III) porphyrin π-cation radical spectrum observed at 293 K into a more complex pattern at 203 K corresponding to three different cation radical species remaining in equilibrium. A substoichiometric amount of 2,4,6 collidine (1:0.5 molar ratio) shifted the acid−base equilibria and the relative concentration of the particular iron(III) porphyrin π-cation radical forms. This observation points out that 2,4,6-collidine acts mainly as a proton scavenger. In addition, separate resonances of the new intermediates **2**-2′ and **3**-2 are readily detected (Figure 4). The resonances are labeled in accord with previously determined assignments. The formation of **2**-2′ is verified by the presence by two pyrrole, ortho, meta, and *p*-CH$_3$

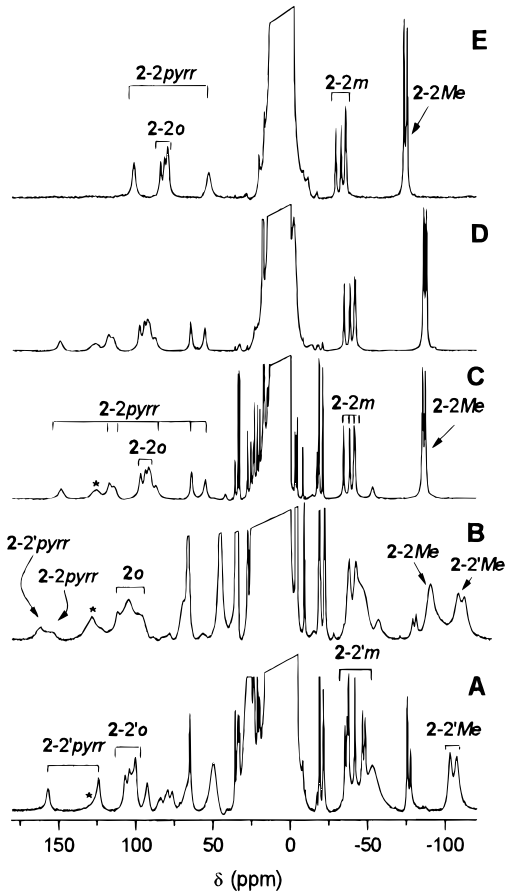

Figure 4. 300 MHz ^{1}H NMR spectra of a dichloromethane-d_2 solution of (TTP$^{\bullet}$)Fe^{III}(ClO$_4$)$_2$ after addition of (A) 0.5 equiv of 2,4,6-collidine, (B) 1 equiv, or (C) 2 equiv of 2,4,6-collidine in dichloromethane-d_2 at 202 K. Trace D: ^{1}H NMR spectrum for the same solution as in part C but after addition of 0.5 equiv of tetrabutylammonium iodide at 202 K. Trace E: ^{1}H NMR spectrum of the dichloromethane-d_2 solution of (TTP$^{\bullet}$)Fe^{III}(ClO$_4$)$_2$ after addition of 2 equiv of 2,4,6-collidine but measured at 232 K. Compounds are labeled as in the text, and subscripts, as in Figure 1. The resonances without any label are due to iron porphyrin π-cation radicals formed before 2,4,6-collidine addition. The resonance marked by an asterisk in trace A corresponds to high-spin (TPP)Fe^{III}X.

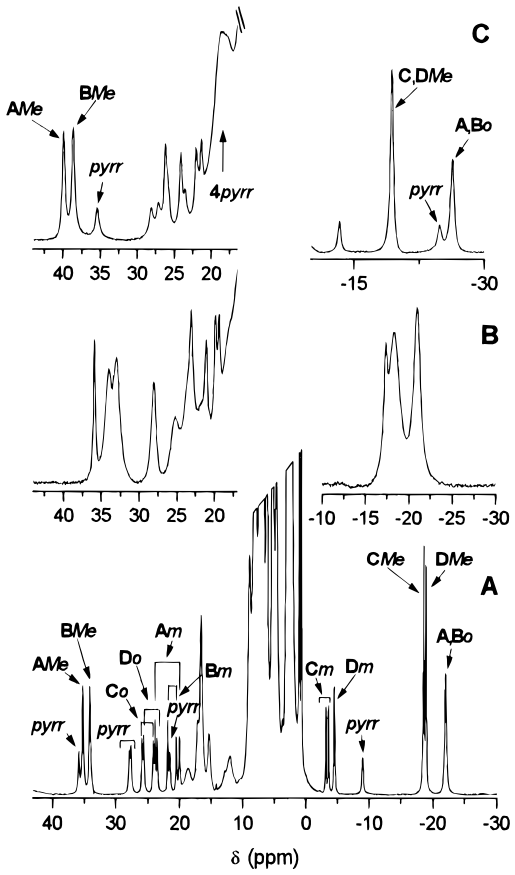

Figure 5. Trace A: Portion of the 300 MHz ^{1}H NMR spectrum of a dichloromethane-d_2 solution of (TTP$^{\bullet}$)Fe^{III}(ClO$_4$)$_2$ after addition of 2 equiv of 2,4,6-collidine in dichloromethane-d_2 at 202 K. Trace B: ^{1}H NMR spectrum of the sample in part A after addition of 0.1 equiv of tetrabutylammonium chloride at 202 K. Trace C: spectrum as in part B but at 176 K. Only resonances of **3**-2 are labeled.

resonances. Other resonances, expected for **2**-2′, are not observed. The reaction mixture composition is dominated by the simple iron porphyrin cation radicals under these conditions. The spectral pattern of this intermediate resembles that one of **2**-1, although the chemical shift values are different. Further titration with 2,4,6-collidine produces gradual growth of a new set of resonances while those of **2**-2′ diminish in intensity (Figure 4). This new form **2**-2 corresponds to the intermediate **2**-1 defined previously for the **1**-1−2,4,6-collidine system. Separate resonances for **2**-2 and **2**-2′ could be observed in whole titration range. Thus, the exchange rate between **2**-2 and **2**-2′ is slow on the ^{1}H NMR time scale. We estimate the rate constant to be much less than 6000 s^{-1}. However the pronounced broadening of **2**-1 and **2**-2′ resonances was noticed during the middle stage of the titration; this observation may indicate a chemical exchange between these two species.

Introduction of 2,4,6-collidine into dichloromethane-d_2 solution of **1**-2 at 202 K generates additional spectral changes which are marked in traces A and B of Figure 4. Figure 5 shows a relevant expansion of the +50 to −30 ppm region of the ^{1}H NMR spectrum. Apart from **2**-2 and **2**-2′, a novel unstable intermediate, **3**-2, has been readily identified during this experiment. The **3**-2 species decays at 223 K and is selectively removed from the reaction mixture by controlled reduction with tetrabutylammonium iodide with the resonances of **2**-2 left intact. The resonances of **3**-2 are clearly seen in Traces A−C of Figure 4 but are missing in the spectrum of the reduced samples (Figure 4, Trace D). The pyrrole resonances of **3**-2 have been assigned by selective deuteration. The comparison of the spectra collected for the (TTP$^{\bullet}$)Fe^{III}(ClO$_4$)$_2$−2,4,6-collidine and (TTP-$d_8^{\bullet}$)Fe^{III}(ClO$_4$)$_2$ systems allows the six pyrrole resonance protons to be identified. It is likely that the two other pyrrole resonances, expected by symmetry considerations, occur under the crowded envelope in the +15 to −5 ppm region. By default, the remaining 20 resonances shifted downfield and upfield are directly assigned to the four inequivalent meso *p*-tolyl groups marked A, B, C, D respectively. The four *p*-methyl resonances have been assigned since they are missing in the spectrum of the phenyl derivative **3**-1. The species **3**-1 has been observed when **1**-1 has been used as the starting material, although in very small concentration. The methyl resonances of **3**-2 have been also identified by integration; each of them had an intensity corresponding to three protons; all other resonances gave one proton intensities in the deconvolution procedures. The two-dimensional COSY experiment is especially effective in the determination of complete sets of resonances which belong to the same meso *p*-tolyl ring (Figure 6). Cross-peaks reveal pairwaise coupling between ortho and meta protons within *p*-tolyl rings. In this experiment we have identified the cross-peaks only for adjacent ortho−meta protons. In the phenyl ring the spin coupling constans follow the order $^3J \gg {}^4J$ and the correlations due to the small couplings, i.e., for the more distant protons are expected to be

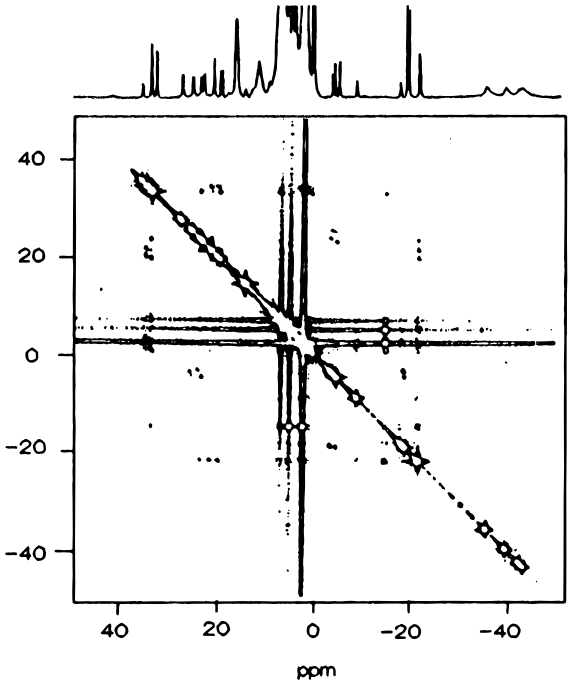

Figure 6. 300 MHz COSY plot for **3**-2 in dichloromethane-d_2 at 202 K. Cross-peaks connecting protons located on the same *p*-tolyl moiety are shown. Assignments of resonaces are as in Figure 5.

very weak.[24] However the distinct cross-peaks have been seen connecting the *p*-methyl group and two adjacent meta protons. This correlation has been used as the starting point in determination of the assignments (Figures 5 and 6; Table 1). The large line widths of pyrrole resonances precluded an observation of their pyrrole-pyrrole cross peaks.

The species **3**-2 can only be observed over the limited temperature range 176−212 K as it undergoes the fast decomposition above 212 K. Plots of the chemical shifts vs $1/T$ reveal that all the resonances for **3**-2 show linear behavior over the relatively narrow accessible temperature range as seen in Figure 7. The extrapolated shifts at the infinite temperature deviate considerably from the anticipated diamagnetic positions.

Treatment of **3**-2 with tetrabutylammonium chloride results in broadening of all resonances as shown in Figure 5 (trace B). The remarkable effect has been seen for the upfield and downfield *p*-tolyl doublets. The corresponding line width values measured for the most downfield shifted pyrrole and *p*-methyl resonances are 65, 73, and 74 Hz and 82, 339, and 246 Hz in the presence and absence of chloride, respectively. This effect can be reversed by lowering the temperature as seen in trace C of Figure 5. We conclude that **3**-2 is involved in axial ligand exchange.

An attempt to follow the processes using selectively deuterated iron(III) cation radicals by ^{2}H NMR in CH_2Cl_2 did not succeed, apparently due to instability of the new intermediates or possibly their precursors in undeuterated solvent, i.e., dichloromethane.

This observation is consistent with the fact that highly oxidized iron porphyrins tend to be more stable in CD_2Cl_2 than in CH_2Cl_2 when the reduction process is considered to involve hydrogen abstraction from the solvent.[12,25,26]

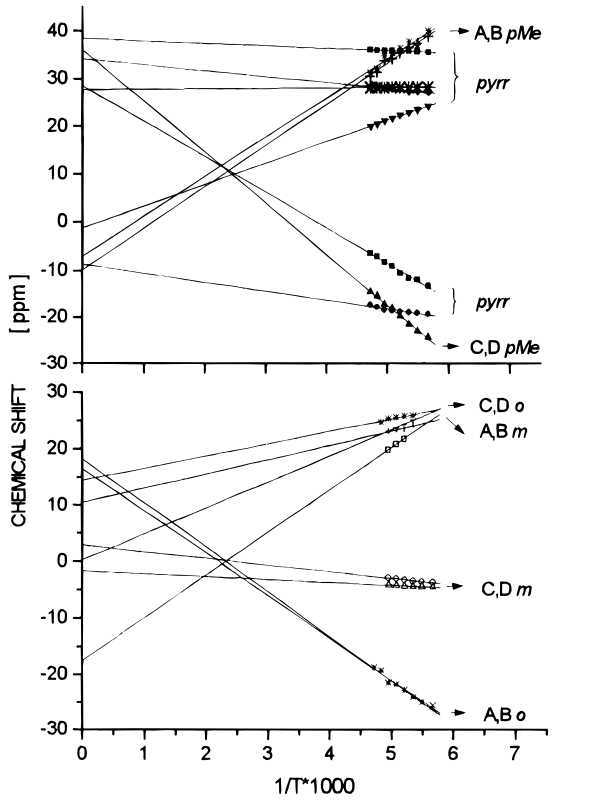

Figure 7. Temperature dependence of chemical shifts for the intermediate **3**-2 formed from (TTP$^{\bullet}$)Fe^{III}(ClO$_4$)$_2$ by addition of 2 equiv of 2,4,6-collidine in dichloromethane-d_2. Solid line shows the extrapolation of the experimental data points as expected from the Curie law. Labels follow those in Figure 1.

Reaction of Iron(III) Tetramesitylporphyrin Cation Radical (TMP$^{\bullet}$)Fe^{III}(ClO$_4$)$_2$ with 2,4,6-Collidine. The ^{1}H NMR spectra of (TMP$^{\bullet}$)Fe^{III}(ClO$_4$)$_2$ **1**-3 were found to be very sensitive to solvent and temperature. Several different cation radical forms were previously recognized by Groves et al. at 203 K in dichloromethane-d_2, toluene-d_8, or dichloromethane-d_2/methanol-d_4.[10] The similar ^{1}H NMR pattern for **1**-3 (dichloromethane-d_2, 203 K) has been reproduced in the experiment carried out in this work. In our opinion coordination of the residual water molecules, followed by acid−base equilibria, results in formation of various iron(III) porphyrin cation radicals of the general formula (TMP$^{\bullet}$)Fe^{III}(X)(Y) (X and Y are available ligands present in the system). Introduction of 1 or 2 equiv of 2,4,6-collidine has clarified the composition with respect to iron(III) porphyrin cation radicals. Only two radical species, labeled **1**-4 and **1**-5 in trace A of Figure 8 prevailed, presumably owing to the increasing contribution of the hydroxy ligand, generated by 2,4,6-collidine in the respective equilibria. Addition of 3 equiv of 2,4,6-collidine has been accompanied by loss of the ^{1}H NMR resonances of iron(III) porphyrin cation radicals and the growth of the new complete set of iron porphyrin resonances. On the basis of a unique spectral pattern the new species has been unambiguously identified as ferryl porphyrin π-cation radical (TMP$^{\bullet}$)Fe^{IV}O(X) (X = monoanion), **5**-1. The formation of **5**-1 has been simultaneously accompanied by the growth of (TMP)Fe^{III}(OH), **6**, resonances.

The complete results of the experiment are given in Figure 8. Further titration with 2,4,6-collidine gradually produced a collection of the **5**-*n* intermediates (Figure 8, trace B). They retain the spectral pattern of the ferryl porphyrin π-cation radical complex although they have significantly different chemical shift values. We attribute these shift changes to axial ligand replacement (Figure 8, Table 1). Essentially only a single form,

(24) Keating, K. A.; de Ropp, J. S.; La Mar, G. N.; Balch, A. L.; Shiau, F.-Y.; Smith, K. M. *Inorg. Chem.* **1991**, *30*, 3258.
(25) Gold, A.; Joyaraj, K.; Doppelt, P.; Weiss, R.; Chottard G.; Bill, E.; Ding, X.; Trautwein, A. X. *J. Am. Chem. Soc.* **1988**, *110*, 5756.
(26) Mizutani, Y.; Hashimoto, S.; Tatsuno, Y.; Kitagawa, T. *J. Am. Chem. Soc.* **1990**, *112*, 6809.

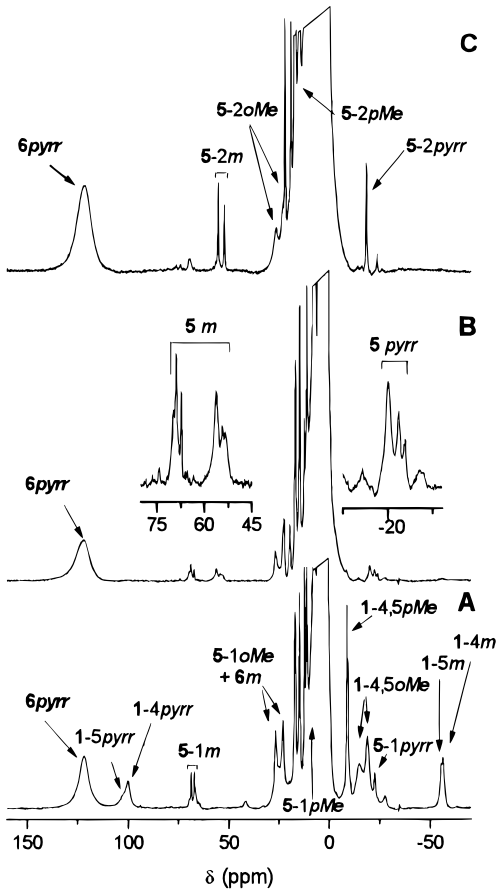

Figure 8. 300 MHz spectra of a dichloromethane-d_2 solution of $(TMP^{\bullet})Fe^{III}(ClO_4)_2$ after addition of (A) 2 equiv, (B) 3 equiv, or (C) 7 equiv of 2,4,6-collidine at 202 K. (Resonances are labeled as in the text.)

5-2, exists for the 1:7 iron porphyrin cation radical:2,4,6-collidine molar ratio. Warming to 293 K has given the stable product **6** and no other iron porphyrin has been detected. Resonance assignments in Figure 8 have been based on relative intensities and comparison with spectra of **5**-2 generated in extensive studies on models of HRP compound I.[10b,15,25,27−30] The pronounced splitting of the *m*- and *o*-methyl resonances is indicative of two different axial ligands in **5**-2. A noticeable axial ligand effect on the ^{1}H NMR spectral parameters has been previously established.[10b,15,30]

These results demonstrate the ability of 2,4,6-collidine to effect the disproportionation process of $(TMP^{\bullet})Fe^{III}(ClO_4)_2$, **1**-3, and/or its hydrated derivatives. The capability to generate highly oxidized ferryl porphyrin cation radicals in the presence of 2,4,6-collidine is of particular significance in light of the reactivity determined for sterically unprotected iron porphyrin cation radicals.

Reaction of Iron(III) Tetra-*p*-tolylporphyrin Cation Radical $(TTP^{\bullet})Fe^{III}(ClO_4)_2$ with 2,6-Substituted Pyridines. Two distinct reactivity patterns of iron(III) porphyrin π-cation radicals in the presence of pyridine and its derivatives have been demonstrated. Previously, an attack of pyridine at the periphery of the porphyrin macrocycle has been determined.[16] Here we have shown that the sterically protected derivative 2,4,6-collidine, which has a limited access to the iron (as a ligand) or to the porphyrin (as a nucleophile), converts the cation radical to new highly oxidized intermediates and subsequently to $[(TPP^{\bullet})Fe^{III}OFe^{III}(TPP)]^+$. To eliminate the possibility that 2,4,6-collidine or any of its feasible transformation products are directly involved in the structure of the new intermediates **2** and **3**, we have decided to explore other 2- or 2,6-substituted pyridines as potential reagents in the investigated processes. The following derivatives have been tested: 2-picoline, 2,6-di-*tert*-butylpyridine, 2,3,6-collidine, and 2,6-dibromopyridine. The bulkness and the chemical properties of the substituents vary to a considerable extent in the series. Careful examination of the ^{1}H NMR spectra (not shown) of the reaction products, obtained for **1**-1−alkylated-pyridine (2-picoline, 2,6-di-*tert*-butylpyridine, 2,3,6-collidine) systems in dichloromethane-d_2 allowed us to identify the intermediates **2**-2 and **3**-2 which are spectroscopic identical to those generated previously by 2,4,6-collidine.

These series of experiments rule out completely the hypothesis that hindered sterically pyridine derivatives might interact directly with iron porphyrin fragment to give new intermediates. In general, the use of the 2,4,6-collidine offers the optimal conditions to form intermediates of interest. Contrary to alkyl substituted pyridines, 2,6-dibromopyridine is inert toward the iron porphyrin π-cation radical. The steric hindrance in this case is expected to be similar as for 2,4,6-collidine. However 2,6-dibromopyridine is the weakest base in the series explored (pK_b decreases in the series 2,4,6-collidine ≈ 2,3,6-collidine > 2-picoline > 2,6-di-*tert*-butylpyridine > 2,6-dibromopyridine).[31] This observation confirms the previous suggestion that the substituted pyridines act mainly as well-tuned proton scavengers.

Reactivity of Novel Intermediates. The species **2**-2 and **3**-2 undergo reduction when treated with triphenylphosphine as shown in Figure 9. Trace A shows the ^{1}H NMR spectrum of **2**-2 and **3**-2 at 203 K prepared as described above. Trace B shows the ^{1}H NMR spectrum of the sample after addition of 0.2 equiv of triphenylphosphine (number of equivalents is given regarding the starting cation radical). The resonances of **3**-2 have diminished in their intensities with respect to these of **2**-2 when 0.2 equiv was added and have disappeared from the spectrum when the next portion of phosphine (0.3 equiv) was added. At this stage the resonances of **2**-2 were still apparent. The reaction is complete in the presence of 0.5 equiv of triphenylphosphine. During the course of the reaction new pyrrole resonances of the reduction products appeared at 130 and −24.7 ppm. The first one corresponds to high-spin iron(III) porphyrins $(TTP)Fe^{III}X$ (anionic ligands available in the reaction environment OH^-, Cl^-) and the second one to low-spin iron(III) tetra-*p*-tolylporphyrin coordinated by triphenylphosphine $[(TTP)Fe^{III}(PPh_3)_2]^+$, **7**. For the sake of comparison, the $[(TTP)Fe^{III}(PPh_3)_2]^+$ model complex, analogous to the previously synthesized $[(TPP)Fe^{III}(PMe_3)_2]^+$,[32] has been independently generated from $(TTP)Fe^{III}(ClO_4)$ and triphenylphosphine at 202 K in dichloromethane-d_2 (trace D of Figure 9). The ^{31}P NMR investigation has demonstrated that triphenylphosphine has been converted into the corresponding triphenylphosphine oxide in the course of the reaction with **2**-2 and **3**-2 (spectra not shown). The measurement has been carried out for the completely reduced sample where 0.5 equiv of PPh_3 reacted. Pyridine-d_5 has been introduced in excess to the system in order to remove the triphenylphospine or triphenylphosphine oxide from the coordination sphere of the iron(III). This precaution has reduced the plausible paramagnetic broadening

(27) Groves, J. T.; Haushalter, R. C.; Nakamura, M.; Nemo, T. E.; Evans, B. J. *J. Am. Chem. Soc.* **1981**, *103*, 284.
(28) Mandon, D.; Weiss, R.; Jayaraj, K.; Gold, A.; Terner, J.; Bill, E.; Trautwein, A. X. *Inorg. Chem.* **1992**, *31*, 4404.
(29) Fujii, H. *J. Am. Chem. Soc.* **1993**, *115*, 4641.
(30) Gross, Z.; Nimri, S. *Inorg. Chem.* **1994**, *33*, 1731.
(31) Perrin, D. In *Dissociation Constants of Organic Bases in Aqueous Solution*; Butterworth: London, 1965.
(32) Simonneaux, G.; Sodano, P. *Inorg. Chem.* **1988**, *27*, 3956.

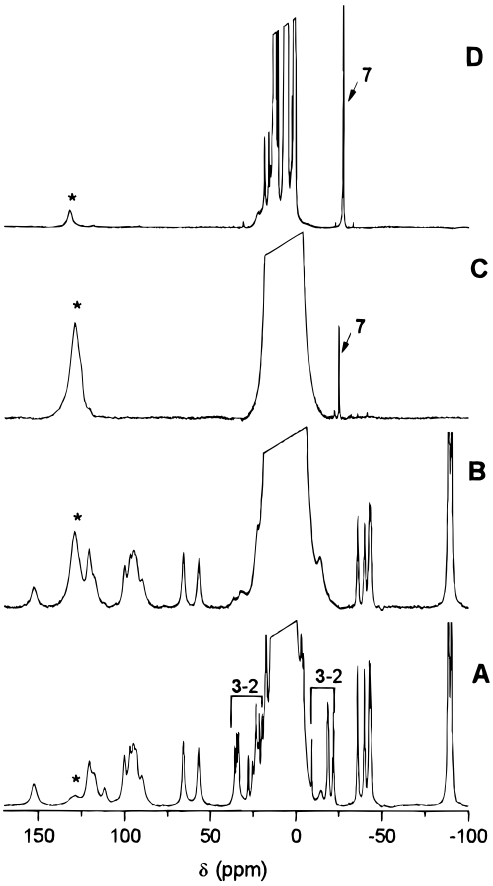

Figure 9. 300 MHz ^{1}H NMR spectra of a dichloromethane-d_2 solution of (TTP$^{\bullet}$)Fe^{III}(ClO$_4$)$_2$ and 2 equiv of 2,4,6-collidine in dichloromethane-d_2 at 202 K after the addition of (A) 0 equiv, (B) 0.2 equiv, or (C) 0.3 equiv of triphenylphosphine. Trace D: ^{1}H NMR spectrum of a solution of (TTP)Fe^{III}(ClO$_4$) and 1 equiv of triphenylphosphine at 202 K in dichloromethane-d_2. The pyrrole resonances of the high-spin iron(III) tetraphenylporphyrin products are marked by an asterisk.

of ^{31}P resonances. The quantity of oxide obtained in the experiment could not be measured in relation to the active form because the reaction mixture was rather complex. Altogether 0.1 equiv of triphenylphosphine oxide was produced from 0.5 equiv of triphenylphosphine. In control ^{1}H and ^{31}P NMR experiments we have established that triphenylphosphine is capable of reacting with (TTP$^{\bullet}$)Fe^{III}(ClO$_4$)$_2$ in the absence of 2,4,6-collidine to produce triphenylphosphine oxide and other unidentified yet phosphine derivatives. The β-substituted product of this reaction (β-PPh$_3$-TTP)Fe^{III}Cl$_2$ was characterized in detail previously.[9]

Significantly, the **2**-2 intermediate has been identified, although in very low concentration, during this reaction. The formation of **2**-2 preceded the complete reduction of the starting radical to high-spin and low-spin iron(III) species including β-substituted ones.[33]

Reduction of **2**-2 and **3**-2 with the one electron reducing reagent tetrabutylammonium iodide proceeds gradually. In the first stage, the **3**-2 intermediate is reduced; in the second stage, **2**-2 reacted (trace D in Figure 4). In the presence of I$^-$ in excess, the (TPP)Fe^{III}X (X ligands available in solution) and [(TTP)Fe^{III}]$_2$O have been identified by means of ^{1}H NMR spectroscopy. The profound asymmetry of **2**-2 and **3**-2 is not preserved in the reduction products. Addition of dichlorine to the solution containing **2**-2 and **3**-2 does not change the number of species in the system (spectra not shown). However, we have observed changes in the relative intensities **3**-2 with respect to **2**-2 as measured by integration. The molar ratio of **2**-2 to **3**-2 varied from 7.2 (no dichlorine added) to 1.2 (after addition ca. 2 equiv of dichlorine). Dibromine is not a sufficiently strong oxidant to effect the oxidation of **2**-2. The results presented here show that **2**-2 undergoes oxidation to produce **3**-2. The process is reversible. Titration of **2**-2 and **3**-2 with TFA or dichloromethane solution of gaseous HCl did not result in any characteristic changes probably due to buffering properties of the 2,4,6-collidine present. Finally both intermediates are stable in the presence of 10 equiv of hexene at 202 K.

(33) Rachlewicz, K.; Latos-Grażyński, L. Unpublished results.

Discussion

The observation of the solution behavior of iron(III) porphyrin π-cation radicals (TPP$^{\bullet}$)Fe^{III}(ClO$_4$)$_2$; (TTP$^{\bullet}$)Fe^{III}(ClO$_4$)$_2$, and (TMP$^{\bullet}$)Fe^{III}(ClO$_4$)$_2$ in the presence of 2,4,6-collidine reveals that these complexes undergo hydration processes which are essential in the generation of highly oxidized species via acid−base equilibria of coordinated water followed by a disproportionation pathway. The reaction routes are influenced by the steric protection granted by the ortho substituents of the meso phenyl rings; for this reason (TTP$^{\bullet}$)Fe^{III}(ClO$_4$)$_2$ and (TMP$^{\bullet}$)Fe^{III}(ClO$_4$)$_2$ cases will be discussed separately.

Reaction of Iron(III) Tetramesitylporphyrin Cation Radical. Several pathways have been explored to generate (X)(TMP$^{\bullet}$)Fe^{IV}O since such a species is considered to model active state of P-450 monooxygenase and has been invoked in mechanism of iron porphyrin based catalysts. The oxidation of iron(III) porphyrins with iodozobenzene, peroxyacids, and ozone resulted in the formation of X(TMP$^{\bullet}$)Fe^{IV}O. Chemical oxidation of (TMP)Fe^{IV}O gave identical highly oxidized products.[15,17,30] The disproportionation of (TMP$^{\bullet}$)Fe^{III}(ClO$_4$)$_2$ in the presence of 1 equiv of methoxide to produce (CH$_3$O)(TMP$^{\bullet}$)Fe^{IV}O was briefly reported.[10b] Recently Groves et al. suggested disproportionation of (TMP)Fe^{IV}O to contribute in the major pathway for olefin oxidation, although existence of this species in the system was not directly shown.[12]

Here the formation of X(TMP$^{\bullet}$)Fe^{IV}O **5** from (TMP$^{\bullet}$)Fe^{III}(ClO$_4$)$_2$ in the presence of 2,4,6-collidine has been unambiguously determined by ^{1}H NMR spectroscopy. The disproportionation reaction is suggested to proceed in the following way:

$$(X)(TMP^{\bullet})Fe^{III}(H_2O) + coll \rightarrow (X)(TMP^{\bullet})Fe^{III}(OH) + collH^+ \quad (1)$$

$$(X)(TMP^{\bullet})Fe^{III}(OH) + coll \rightarrow \{(X)(TMP^{\bullet})Fe^{III}(O^-)\} + collH^+ \quad (2)$$

$$\{(X)(TMP^{\bullet})Fe^{III}(O^-)\} \rightarrow (TMP)Fe^{IV}O + X^- \quad (3)$$

$$\mathbf{(TMP)Fe^{IV}O} + (X)(Y)(TMP^{\bullet})Fe^{III} \rightarrow \mathbf{(Y)(TMP^{\bullet})Fe^{IV}O} + (TMP)Fe^{III}X \quad (4)$$

An alternative pathway includes the contribution of the iron(IV) hydroxy species

$$(X)(TMP^{\bullet})Fe^{III}(OH) \rightarrow (X)(TMP)Fe^{IV}(OH) \quad (5)$$

$$2(X)(TMP)Fe^{IV}(OH) + coll \rightarrow (X)(TMP^{\bullet})Fe^{IV}(O) + (TMP)Fe^{III}(OH) + collH^+ + X^- \quad (6)$$

At present we cannot identify any of species preceding (X)(TMP$^{\bullet}$)Fe^{IV}(O), **5**-*n*, in the reaction sequence due to their inherent instability in the presence of strongly oxidizing iron-

(III) porphyrin cation radicals.[15] The summary of the disproportionation reaction is

$$2(X)(TMP^{\bullet})Fe^{III}(OH) + coll \rightarrow (X)(TMP^{\bullet})Fe^{IV}O + (TMP)Fe^{III}(OH) + collH^{+} + X^{-} \quad (7)$$

We postulate that $(X)(TMP^{\bullet})Fe^{IV}O$, once formed, undergoes a typical decay via abstraction of the hydrogen from the solvent.[12,25,26] This final path leads to $(TMP)Fe^{III}(OH)$ **6** and/or $(TMP)Fe^{III}X$ as demonstrated experimentally. The reactivity of $(X)(TMP^{\bullet})Fe^{III}(H_2O)$ in the presence of 2,4,6-collidine points out the special role of this pyridine derivative as an effective and oxidation-resistant proton scavenger which can be explored in this function for other hydrated iron porphyrin π-cation radicals.

Reactions of Iron(III) Tetraphenylporphyrin and Iron(III) Tetra-*p*-tolylporphyrin Radical. The reactivity pattern observed for $(TPP^{\bullet})Fe^{III}(ClO_4)_2$, **1**-1, and $(TTP^{\bullet})Fe^{III}(ClO_4)_2$, **1**-2, stimulated by 2,4,6-collidine as the efficient proton scavenger, differ in several significant ways from those of $(TMP^{\bullet})Fe^{III}(ClO_4)_2$, **1**-3. As the representative for **1**-1 and **1**-2, the reactivity of **1**-2 is discussed in detail. The iron porphyrin π-cation radical **1**-2 in the presence of 2,4,6-collidine has generated novel detectable intermediates **2**-2**,** **2**-2′, and **3**-2. Their formation has been accompanied by the final iron(III) product, i.e. $[(TTP^{\bullet})Fe^{III}OFe^{III}(TTP)\}^{+}$, **4**-2. These novel intermediates are highly asymmetric and extremely unstable and have been observed only at low temperature. Unlike sterically hindered **1**-3, there is no spectroscopic evidence for the formation of the highly oxidized ferryl porphyrin π-cation radical $X(TTP^{\bullet})Fe^{IV}O$. Only with a high degree of the steric protection available for $X(TMP^{\bullet})Fe^{IV}O$, **5**, could such an intermediate be detected by ^{1}H NMR at low temperature.[10,15,17,27−30,34] A large variety of highly oxidized intermediates may be implied in the reaction mechanisms under highly oxidizing conditions ($Fe^{IV}O$ porphyrin π-cation radical, $Fe^{V}O$ porphyrin, Fe^{III} porphyrin dication and Fe^{III} porphyrin *N*-oxide).[18,35,36] In particular, experimental as well as theoretical studies have suggested that the reactive forms of highly oxidized iron porphyrins involved in oxygen activation and heme destruction may contain a structure in which an oxygen atom is inserted into N−Fe bond as an alternate to the more conventional oxoiron structure.[37−40] This is the only form which may impose an asymmetry on porphyrin skeleton.

The newly detected species **2**-2 and **3**-2 demonstrated the unprecedented ^{1}H NMR spectral patterns bearing the closest resemblance to iron complexes of N-substituted tetraarylporphyrin in the appropriate electronic/spin states. For the sake of comparison, the relevant spectral parameters are gathered in Table 1. The ^{1}H NMR spectra are indicative of the dramatic reduction of symmetry for **2**-2**,** **2**-2′ and **3**-2 as compared to the effective D_{4h} symmetry of the starting π-cation radical or the C_{4v} symmetry assigned to the two subunits of the diiron product **4**. The ^{1}H NMR spectra of **2**-2 and **3**-2 show large alternating hyperfine shift for the meso aryl substituents that are consistent with the iron porphyrin π-cation radical electronic structure of both intermediates.

Considering these arguments, we have identified **2**-2 and **3**-2 as related to N−O porphyrin derivatives i.e. iron(III) porphyrin *N*-oxide π-cation radical (**2**) and iron(IV) porphyrin *N*-oxide π-cation radical (**3**).

The suggested mechanism of the **2**-2 and **3**-2 formation is as follows:

$$[(X)(TTP^{\bullet})Fe^{III}(H_2O)]^{+} + coll \rightarrow (X)(TTP^{\bullet})Fe^{III}(OH) + collH^{+} \quad (8)$$

$$(X)(TTP^{\bullet})Fe^{III}(OH) + coll \rightarrow \{(X)(TTP^{\bullet})Fe^{III}(O^{-})\} + collH^{+} \quad (9)$$

$$\{(X)(TTP^{\bullet})Fe^{III}(O^{-})\} \rightarrow (TTP)Fe^{IV}O + X^{-} \quad (10)$$

$$\mathbf{(TTP)Fe^{IV}O} + (X)(Y)(TTP^{\bullet})Fe^{III} \rightarrow (X)\mathbf{(TTP^{\bullet})Fe^{IV}O} + (TTP)Fe^{III}Y \quad (11)$$

$$(X)(TTP^{\bullet})Fe^{IV}O \rightarrow TTP\text{-}N{-}O{-}Fe^{III}X \quad (12)$$

$$TTP{-}N{-}O{-}Fe^{III}X - e^{-} \rightarrow [TTP^{\bullet}{-}N{-}O{-}Fe^{III}X]^{+} \quad (13)$$

An alternative pathway includes the contribution of the iron(IV) hydroxy species

$$(X)(TTP^{\bullet})Fe^{III}(OH) \rightarrow (X)(TTP)Fe^{IV}(OH) \quad (14)$$

$$2(X)(TTP)Fe^{IV}(OH) \rightarrow [(X)(TTP)Fe^{V}(OH)]^{+} + (TTP)Fe^{III}(OH) + X^{-} \quad (15)$$

$$[(X)(TTP)Fe^{V}(OH)]^{+} \rightarrow [TTP{-}N{-}O(H){-}Fe^{III}X]^{+} \quad (16)$$

The feasible route involves iron(III) porphyrin dication species

$$[(X)(TTP)Fe^{V}(OH)]^{+} \leftrightarrow [(X)(TTP^{2+})Fe^{III}(OH)]^{+} \quad (17)$$

$$[(X)(TTP^{2+})Fe^{III}(OH)]^{+} \rightarrow [TTP{-}N{-}O(H){-}Fe^{III}X]^{+} \quad (18)$$

$$[TTP{-}N{-}O(H){-}Fe^{III}X]^{+} + coll \rightarrow TTP{-}N{-}O{-}Fe^{III}X + collH^{+} \quad (19)$$

and, at the final stage

$$TTP{-}N{-}O{-}Fe^{III}X - e^{-} \rightarrow [TTP^{\bullet}{-}N{-}O{-}Fe^{III}X]^{+} \quad (20)$$

$$TTP^{\bullet}{-}N{-}O{-}Fe^{III}X - e^{-} \rightarrow [TTP^{\bullet}{-}N{-}O{-}Fe^{IV}X]^{2+} \quad (21)$$

In all reaction X corresponds to available axial ligands which are water, hydroxy anion, and perchlorate. The iron(III) porphyrin cation radicals act also as efficient one-electron oxidizing reagents. Highly oxidized intermediates, once formed, undergo a typical decay via abstraction of the hydrogen from the solvent. This routes leads to $(TTP)Fe^{III}(OH)$ and $[(TTP^{\bullet})Fe^{III}(OH)]^{+}$ which finally react as given in eq 22. The TTP−

$$(TTP)Fe^{III}(OH) + [(TTP^{\bullet})Fe^{III}(OH)]^{+} \rightarrow [(TTP^{\bullet})Fe^{III}OFe^{III}(TTP)]^{+} + H_2O \quad (22)$$

N−O−Fe^{III}X form, although postulated in the reaction sequence,

(34) Mandon D.; Weiss, R.; Franke, M.; Bill, E.; Trautwein, A. X. *Angew. Chem., Int. Ed. Engl.* **1989**, *28*, 1709.
(35) Watanabe, Y.; Takehira, K.; Shimizu, M.; Hayakawa, T.; Orita, H.; Kaise, M. *J. Chem. Soc., Chem. Commun.* **1990**, *18*, 1262.
(36) Yamaguchi, K.; Watanabe, Y.; Morishima, I. *J. Chem. Soc., Chem. Commun.* **1992**, 1771.
(37) (a) Bonnett, R.; Ridge, R. J.; Appelman, E. H. *J. Chem. Soc., Chem. Commun.* **1978**, 310. (b) Andrews, L. E.; Bonnett, R.; Ridge, R. J.; Appelman, E. H. *J. Chem. Soc., Perkin Trans. 1* **1983**, 103.
(38) (a) Latos-Grażyński, L; Cheng, R.-J.; La Mar, G. N.; Balch, A. L. *J. Am. Chem. Soc.* **1981**, *103*, 4270. (b) Olmstead, M. M.; Cheng, R.-J.; Balch, A. L. *Inorg. Chem.* **1982**, *21*, 4143. (c) Balch, A. L.; Chan, Y.-W.; Olmstead, M. M.; Renner, M. W. *J. Am. Chem. Soc.* **1985**, *107*, 2393. (d) Balch, A. L.; Chan, Y.-W.; Olmstead M. M. *J. Am. Chem. Soc.* **1985**, *107*, 6510.
(39) Chevrier, B.; Weiss, R.; Lange, M.; Chottard, J. C.; Mansuy, D. *J. Am. Chem. Soc.* **1981**, *103*, 2899.
(40) (a) Tatsumi, K.; Hoffmann, R. *Inorg. Chem.* **1981**, *20*, 3771. (b) Strich, A.; Veillard, A. *Nouv. J. Chim.* **1983**, *7*, 347.

could not be directly observed. The analogous TTP−N−O−$Fe^{III}X$ was not detectable by ^1H NMR spectroscopy because pyrrole resonances were extremely broad.[21] In addition in the highly oxidizing condition the complete conversion to the one- or two-electron oxidized derivatives could take place.

Further suggestions for the formulation of **2** and **3** as $[TTP^{\bullet}-N-O-Fe^{III}X]^+$ and $[TTP^{\bullet}-N-O-Fe^{IV}X]^{2+}$ respectively come from their mutual conversion **2**-2 → **3**-2 by addition of the external oxidizing agent Cl_2 and **3**-2 → **2**-2 by addition of the external reducing reagent iodide. This allows reversal of reaction 21 in a controlled manner. This transformation indicates that the fundamental porphyrin *N*-oxide skeleton is preserved in both species. The reactivity toward the standard oxygen atom acceptors is also in accord with the porphyrin *N*-oxide formulation. The intermediates **2**-2 and **3**-2 are stable in the presence of olefins at 203 K. It this context it should be noted that the (TMP−N−O−$Fe^{III}X$ complex is also not effective in the epoxidation of olefins.[21] However both intermediates are finally reduced to iron(III) porphyrins upon treating with triphenylphosphine. The detection of phosphine oxide as a product demonstrates the ability of **2**-2 and **3**-2 to act as an oxygen atom transfer agent:

$$[TTP^{\bullet}-N-O-Fe^{III}X]^+ + PPh_3 \rightarrow [(TTP^{\bullet})Fe^{III}X]^+ + OPPh_3 \quad (23)$$

$$[TTP^{\bullet}-N-O-Fe^{IV}X]^{2+} + PPh_3 \rightarrow [(TTP^{\bullet})Fe^{IV}X]^{2+} + OPPh_3 \quad (24)$$

Both iron porphyrin products of the reaction may repeatedly contribute in the overall reaction route. At present the identification of **2**-2′, which precedes formation of **2**-2, is even more limited. The simultaneous dynamic broadening of two **2**-2 and **2**-2′ sets of resonances has been also demonstrated in the intermediate point of the titration with 2,4,6-collidine. Two processes related to the acid−base equilibrium are relevant in this case. The protonation of **2**-2 to obtain **2**-2′ or **2**-2″ might be located either at N−O (eqs 25 and 26) or on the OH ligand (eq 27).

$$TTP^{\bullet}-N-O(H)-Fe^{III}X\ (\mathbf{2}\text{-}2') + coll \rightleftharpoons TTP^{\bullet}-N-O^{-}-Fe^{III}X + collH^+ \quad (25)$$

$$TTP^{\bullet}-N-O^{-}-Fe^{III}X \rightleftharpoons TTP^{\bullet}-N-O-Fe^{III}X \quad (26)$$

$$TTP^{\bullet}-N-O-Fe^{III}(H_2O)\ (\mathbf{2}\text{-}2'') \rightleftharpoons TTP^{\bullet}-N-O-Fe^{III}(OH) \quad (27)$$

Taken as a whole these results strongly suggest that **2** and **3** complexes contain the porphyrin *N*-oxide ligand. Formally **2** and **3** species are oxidized by three or four electrons about the iron(III) porphyrin level. Two oxidizing equivalents are absorbed by the N-substitution (eqs 12 and 18). One electron oxidation of the macrocycle (eq 20), accompanied by one electron oxidation of the iron(III) to iron(IV) (eq 21), are responsible for the storage of two other equivalents.

There exists significant parallel in the complexes that iron forms with *N*-methyltetraarylporphyrins[22,23] and porphyrin *N*-oxides (Table 1).[21] Recently two different highly oxidized iron complexes of *N*-methyltetra-*p*-tolylporphyrin were detected by ^1H NMR spectroscopy, formally oxidized by three or four electrons above the ground state of iron(III) porphyrin.[23] It was also demonstrated that one of the intermediates was oxidized to a *N*-methylporphyrin π-cation radical.[23]

Electronic Structure. The ^1H NMR spectrum of **2** is readily informative of two aspects of the electronic structure. The sizable hyperfine shifts observed for the meso aryl substituents of the porphyrin along with pattern of these shifts indicate that modified ligand has been oxidized to a porphyrin π-cation radical. The alternating signs for the chemical shifts for the ortho and para vs the meta aryl protons and the change of signs of the shift that occurs upon substituting a methyl group for a proton are consistent with a π mechanism of spin delocalization into the meso substituents from meso carbon. The spectral pattern reported for $(TPP^{\bullet})Fe^{III}Cl((SbCl_6)$ is very similar to that of **2**.[41] Even stronger similarities as far as the extent of spin delocalization is concern have been noticed for iron *N*-methyltetra-*p*-tolylporphyrin π-cation radical although the pattern of detected *p*-tolyl resonances is reversed here.[23] The observation of strongly downfield shifted pyrrole resonances in the region typical for high-spin iron(III) tetraarylporphyrins and high-spin iron(III) N-substituted tetraarylporphyrins is consistent with a high spin iron(III) electronic structure of **2**.[22,23,42] In this electronic state the $d_{x^2-y^2}$ orbital is half-occupied and the contact contribution produces large downfield shifts for unsubstituted pyrrole resonances via the σ-mechanism. The overall pattern of the isotropic shifts for high-spin iron(III) porphyrin π-cation radicals reflects a convolution of those two spin distribution mechanisms preserving the direction and size of pyrrole shifts with the direction of phenyl resonance reflecting the ferromagnetic vs. antiferromagnetic interaction.[41]

The ^1H NMR data for **3** show a number of remarkable features that must arise from its unusual molecular and electronic structure. The *p*-tolyl resonances are divided in two distinct sets. In the first set the *p*-tolyl groups show downfield shift for ortho and upfield for *m*- and *p*-methyl protons, in the second one the pattern is reversed: ortho protons are shifted upfield but *m*- and *p*-methyl protons downfield. The observed pyrrole resonances demonstrated also downfield and upfield shifts. Thus the available data indicate that the signs of the spin densities on two meso positions are opposite those on the other two meso positions. The same observation is valid for the pyrrole positions. The pattern of *p*-tolyl resonaces is consistent with cation radical electronic structure of **3**.

The observed hyperfine shifts reflect the lowering symmetry and the simultaneous contribution of the iron and porphyrin radical to the contact shifts. It can be concluded that the odd patterns for the contact shift in **3** arise from addition of the effects of unpaired spin density of opposite signs but similar absolute value resulting from the spin density localization in orbitals related to 3e(π), 4e(π), a_{1u} and a_{2u} orbitals of D_{4h} symmetry. The geometry dependent magnetic coupling between the iron and porphyrin centers additionally complicates the matter.[41]

Two extremal cases of π-cation radicals have been characterized for metalloporphyrins of D_{4h} symmetry.[4,43] The a_{2u} radical places the positive spin density at meso and nitrogen positions. In contrast, the a_{1u} radical locates the spin density at the α- and β-pyrrole carbons and via correlation the negative spin density at meso position. It was estimated that this spin density may result in −200 and +109 ppm limiting shifts in both available electronic structures at 295 K.[43] The thermal equilibrium between a_{2u} and a_{1u} states can modulate the size and sign of the contact shift for meso protons or meso phenyls of cation radicals.[44,45]

(41) Gans, P.; Buisson, G.; Duwe, E.; Marchon, J.-C.; Erler, B. S.; Scholz, W. F.; Reed, C. A. *J. Am. Chem. Soc.* **1986**, *108*, 1223.
(42) Artaud, I.; Gregoire, P.; Leduc, P.; Mansuy, D. *J. Am. Chem. Soc.* **1990**, *112*, 6899.
(43) Phillippi, M. A.; Goff, H. M. *J. Am. Chem. Soc.* **1982**, *104*, 6026.

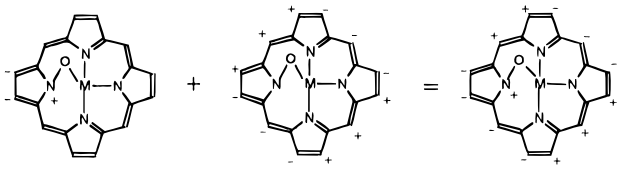

Figure 10. Idealized distortion modes for the porphyrin macrocycle: (A) mode angling one of the pyrrole rings, (B) ruffled distortion, (C) convolution of angling and ruffling. Displacement of the atoms with respect to the least-square porphyrin plane are shown as + = above the plane and − = below the plane.

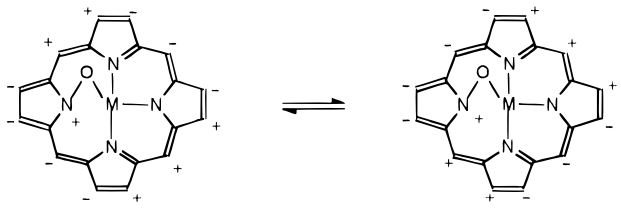

Figure 11. Representation of the macrocyclic inversion process for the two suggested conformations of **2** and **3**. Displacement of the atoms with respect to the least-square porphyrin plane are shown as + = above the plane and − = below the plane.

If a_{1u} and a_{2u} related orbitals of the radical **3** impose internal heterogeneous spin density distribution at meso positions and the sign of the spin density is different for each orbital, the thermal equilibrium between a_1 and a_2 states may account for encountered sign variation at meso positions. However in the absence of the more detailed information on the electronic/spin state of iron any more detailed interpretation of the spin density distribution mechanizm would be too speculative.

Rearrangement Mechanism. To account for the asymmetry of **2** and **3** porphyrin skeletons and the dynamic process detected in variable temperature measurements we have analyzed the molecular structure of the several N-substituted or metal ion−nitrogen inserted porphyrin derivatives.[38,46,47] The pyrrole to which a substituent has been added is usually sharply angled out of the plane of the porphyrin. Some puckering of the residual part of the N-substituted porphyrin was also observed.[22,46,47] Typically the solid state structure demonstrates also inequivalence of each porphyrin position. However, if the N-substituent is symmetrical an effective C_s symmetry is usually demonstrated in solution by ^{1}H NMR spectra.[22b,38] The asymmetric derivative iron porphyrin with an asymmetric vinylidene carbene inserted into an iron−nitrogen bond produced doubling of all pyrrole resonances.[42] There exists a large set of structural data which shows that even the non-N-substituted symmetrically substituted porphyrin macrocycle is conformational flexible and capable of adopting a nonplanar conformation in the solid state and in solution.[48] Significant skeletal puckering has been also observed in a variety of metallotetraarylporphyrin radicals.[41,48] Two idealized saddle and ruffled distortion modes for the porphyrin macrocycle in the D_{2d} symmetry are usually considered.[48−50] We assume that the distortion of the porphyrin macrocycle in **2** and **3** may be approximated by a resultant of the structural consequence of oxygen insertion and ruffling as shown schematically in Figure 10. Two enantiomeric structures can be differentiated by the orientation of ruffling. The pairwaise broadening followed by the collapsing has been observed for the pyrrole resonances of **2** (Figures 1, 2, and 4). Such a dynamic behavior indicates that the mechanism of the chemical exchange process involves a conversion from one enatiomer to another as shown in Figure 11. The coalescence temperature T_c can be used to calculate the free energy of activation for the pyrrole resonances of **2** to become equivalent by using the standard equation $\Delta G^{\ddagger} = RT_c\,(22.96 + \ln(T_c/\delta\nu)$.[51] The free enthalpy of activation of the conformational process at question has been estimated at the coalescence point temperature for the pyrrole couple centered at 60 ppm at 202 K. The corresponding resonances are narrowest and presented the most pronounced separation in the temperature region preceding the dynamic behavior. The required shift difference $\delta\nu$ has been determined by extrapolating this value from the 180−202 K temperature range, assuming the Curie dependence of the paramagnetic shifts.

For a coalescence temperature of 220 K established for **2**-2 this calculation yields a value $\Delta G^{\ddagger} = 9.0$ kcal/mol. Similar value has been obtained for **2**-1 with $\Delta G^{\ddagger} = 8.8$ kcal/mol at $T_c = 210$ K. The $\Delta G^{\ddagger}$ value calculated for **2** is in the limit typical for rearrangement processes found for metalloporphyrin macrocycles which involve inversion of saddle or ruffled structures.[49,50]

The unique distribution of the spin density in **2** and **3** has to be related to the ruffled structure of the porphyrin in analogy to significant differences in spin delocalization observed for the puckered porphyrin cation radical as compared to the planar porphyrin cation radical.[52,53] The conformational puckering tends to shift spin density onto the phenyl ring. This trend probably arises from the fact that the phenyl rings roll more into the porphyrin plane to minimize steric interaction with β-pyrrolic protons. The efficiency of this contribution which extends the aromacity of the system may be instrumental in stabilization of porphyrin *N*-oxide structure for TTP (TPP) vs TMP where the steric hindrance destabilizes coplanar arrangement of phenyl and porphyrin macrocycles.

Conclusion

The present work offers the strong spectroscopic evidence that the disproportionation reaction of hydrated iron(III) porphyrin π-cation radicals result in formation of novel highly oxidized iron porphyrins. We have established that the new disproportionation route, stimulated by the proton scavenger 2,4,6-collidine of sterically hindered $(TMP^{\bullet})Fe^{III}(ClO_4)_2$, produces a well-characterized ferryl porphyrin π-cation radical. However in the case of unhindered tetraarylporphyrin derivatives we have found the formation of two unprecedented highly oxidized intermediates which have the structures related to porphyrin *N*-oxide. The possibility of oxene insertion into the metal−nitrogen bond has been raised as an alternative for highly oxidized forms of heme proteins (particularly cytochrome P450

(44) (a) Morishima, I.; Shiro, Y.; Takamuki, Y. *J. Am. Chem. Soc.* **1983**, *105*, 6168. (b) Morishima, I.; Takamuki, Y.; Shiro, Y. *J. Am. Chem. Soc.* **1983**, *105*, 6168.
(45) Rachlewicz, K.; Latos-Grażyński, L. *Inorg. Chim. Acta* **1988**, *144*, 213.
(46) Lavallee, D. K. *The Chemistry and Biochemistry of N-substituted Porphyrins*; VCH Publishers: New York, 1987; p 12.
(47) (a) Callot, H. J.; Chevrier, B.; Weiss, R. *J. Am. Chem. Soc.* **1978**, *100*, 4733. (b) Chevrier, B.; Weiss, R. *J. Am. Chem. Soc.* **1976**, *98*, 2985.
(48) Scheidt, R. W.; Lee, Y. *Struct. Bonding* **1987**, *64*, 1.
(49) Barkigia, K. M.; Berber, M. D.; Fajer, J.; Medforth, C. J.; Renner, M. W.; Smith, K. M. *J. Am. Chem. Soc.* **1990**, *112*, 8851.
(50) Medforth, C. J.; Senge, M. O.; Smith, K. M.; Sparks, L. D.; Shelnutt, J. A . *J. Am. Chem. Soc.* **1992**, *114*, 9859.
(51) Abraham, R. J.; Fisher, J.; Loftus, P. In *Introduction to NMR Spectroscopy*; Wiley and Sons: Chichester, England, 1988.
(52) Renner, M. W.; Cheng, R.-J.; Chang, C.; Fajer, J. *J. Phys. Chem.* **1990**, *94*, 8508.
(53) Sparks, L. D.; Medforth, C. J.; Park, M.-S.; Chamberlain, J. R.; Ondrias, M. R.; Senge, M. O.; Smith, K. M.; Shelnutt, J. A. *J. Am. Chem. Soc.* **1993**, *115*, 581.

and the peroxidases) and as intermediates in heme catabolism. In this respect shift of an oxene unit from metal to nitrogen, considered here as a possible step in the formation of new intermediates **2** and **3** can be also essential for heme oxidase activity. Oxygen migration from metal to meso position may account for hydroxylation processes. It will be interesting to determine if previously unconsidered porphyrin *N*-oxide π-cation radical intermediates are of importance in such a transfer.

Nevertheless it is clear from the present studies that ligand-centered oxidation occurs in **2** and **3** and that both posses remarkable electronic and molecular structures. This work continues to emphasize that N-substituted porphyrins and normal porphyrins have similar abilities to stabilize corresponding spin/oxidation/ligation states of iron. The role of these oxidized species in the oxygen atom transfer remains to be explored.

Experimental Section

Tetraphenylporphyrin ($TPPH_2$), tetra-*p*-tolylporphyrin ($TTPH_2$), and tetramesitylporphyrin ($TMPH_2$) and the respective deuterated derivatives ($TPPH_2$-d_8, $TPPH_2$-d_{20}, and $TTPH_2$-d_8) were prepared using reported methods.[7,54,55] Insertion of iron into these porphyrins followed known routes.[56]

2-Picoline, 2,6-di-*tert*-butylpyridine, 2,3,6-collidine, and 2,6-dibromopyridine were used as received from Aldrich. 2,4,6-Collidine (Aldrich) was dried and distilled over KOH directly before use. Deuterated solvents ($CDCl_3$ (Glaser AG), CD_2Cl_2 (Aldrich)) used in the reactivity studies of iron porphyrin cation radicals were purified directly before experiments by distillation over CaH_2.

All chemicals were dried prior to use and were stored in the drybox. All solutions in the appropriate solvents were prepared in the drybox and samples were kept in vials or in NMR tubes sealed with septum caps. All transfers have been carried out using a syringe technique.

$(TPP^{\bullet})Fe^{III}(ClO_4)_2$, $(TTP^{\bullet})Fe^{III}(ClO_4)_2$, and $(TMP^{\bullet})Fe^{III}(ClO_4)_2$ were synthesized according to described procedures.[41] One-electron reduction of π-cation radicals with KI resulted solely in a recovery of iron(III) tetraphenylporphyrin derivatives.

Low Temperature Reactivity Studies. The required number of pyridine derivative equivalents were added by a microliter syringe to the sample of the iron(III) porphyrin cation radical in a NMR tube at 193 K. The sample was shaken in the cold bath and transferred to the precooled NMR probe to follow the progress of the reaction.

Instrumentation. ^{1}H NMR spectra were recorded on a Bruker AMX spectrometer operating in the quadrature mode at 300 MHz. A typical spectrum was collected over a 45 000 Hz spectral window with 16 K data points with 500−5000 transients for the experiment and a 50 ms prepulse delay. The free induction decay (FID) was apodized using exponential multiplication depending on the natural line width. This induced 5−50 Hz broadening. The residual ^{1}H NMR spectra of the deuterated solvents were used as a secondary references.

The ^{31}P NMR spectra were collected using a Bruker AMX instrument operating at 121.442 MHz. A spectral width of 20 kHz was typical, and 16K points was used. The signal to noise ratio was improved as in proton spectra. The residual ^{31}P NMR resonance of PPh_3 was used as a secondary reference. The COSY spectrum was obtained after collecting a standard 1D reference spectrum. The 2D spectrum was collected by use of 1024 points in t_2 over the desired bandwidth (to include all desired peaks) with 258 t_1 blocks and 1024 scans per block. All experiments included four dummy scans prior to the collection of the first block. Absorption spectra were recorded on a Specord M-42 spectrophotometer.

Acknowledgment. The financial support of the State Committee for Scientific Research KBN (Grant 2 2651 92 03) is kindly acknowledged.

IC950876K

(54) Lindsey, J. S.; Schreiman, I. C.; Hsu, H. C.; Kearney, P. C.; Marguerettaz, A. M. *J. Org. Chem.* **1987**, *52*, 827.
(55) Boersma, A. D.; Goff, H. M. *Inorg. Chem.* **1982**, *21*, 581.
(56) Adler, A. D.; Longo, F. R.; Kampas, F.; Kim, J. *J. Inorg. Nucl. Chem.* **1970**, *32*, 2443.